Analysis of Cell Membrane Characteristics of In Vitro-Selected Daptomycin-Resistant Strains of Methicillin-Resistant *Staphylococcus aureus*[▽]

Nagendra N. Mishra,[1] Soo-Jin Yang,[1] Ayumi Sawa,[1] Aileen Rubio,[2] Cynthia C. Nast,[3,4] Michael R. Yeaman,[1,4] and Arnold S. Bayer[1,4]*

Division of Infectious Diseases, Los Angeles Biomedical Research Institute at Harbor—University of California at Los Angeles (UCLA) Medical Center, 1124 West Carson St., Torrance, California 90502[1]; Cubist Pharmaceuticals, Lexington, Massachussetts[2]; Cedars-Sinai Medical Center, Los Angeles, California[3]; and David Geffen School of Medicine at UCLA, Los Angeles, California[4]

Our previous studies of clinical daptomycin-resistant (Dap[r]) *Staphylococcus aureus* strains suggested that resistance is linked to the perturbations of several key cell membrane (CM) characteristics, including the CM order (fluidity), phospholipid content and asymmetry, and relative surface charge. In the present study, we examined the CM profiles of a well-known methicillin-resistant *Staphylococcus aureus* (MRSA) strain (MW2) after in vitro selection for DAP resistance by a 20-day serial passage in sublethal concentrations of DAP. Compared to levels for the parental strain, Dap[r] strains exhibited (i) decreased CM fluidity, (ii) the increased synthesis of total lysyl-phosphatidylglycerol (LPG), (iii) the increased flipping of LPG to the CM outer bilayer, and (iv) the increased expression of *mprF*, the gene responsible for the latter two phenotypes. In addition, we found that the expression of the *dlt* operon, which also increases positive surface charge, was enhanced in the Dap[r] mutants. These phenotypic and genotypic changes correlated with reduced DAP surface binding, mirroring observations made in clinical Dap[r] isolates. In this strain, serial exposure to DAP induced an increase in vancomycin MICs into the vancomycin-intermediate *S. aureus* (VISA) range (4 μg/ml) in parallel with increasing DAP MICs. Also, this Dap[r] strain exhibited significantly thicker cell walls than the parental strain, potentially correlating with the coevolution of the VISA phenotype and implicating cell wall structure and/or function in the Dap[r] phenotype. Importantly, despite the overexpression of *mprF* and *dlt*, the relative net positive surface charge was decreased in the Dap[r] mutants, suggesting that other factors contribute to the surface charge alterations and that a simple charge repulsion mechanism could not entirely explain the Dap[r] phenotype in these strains.

Staphylococcus aureus can cause a variety of localized and more invasive infections, especially when the skin or a mucosal barrier is breached (26). Such infections can be particularly problematic when the organism is multiply drug resistant, as in the case of methicillin-resistant *S. aureus* (MRSA). The poor treatment outcomes often associated with serious MRSA infections demonstrates the need for alternative effective treatment options. Daptomycin (DAP) is a lipopeptide antibiotic that was approved for the treatment of gram-positive bacterial infections in 2003 (12, 14, 17). The agent has received much interest because of its activity against multidrug-resistant, gram-positive bacteria such as MRSA, vancomycin-resistant enterococci, and glycopeptide-intermediate and -resistant *S. aureus* (14, 43). While the mode of action of DAP is not entirely clear (30), it is known that calcium-dependent binding to the bacterial CM and the disruption of CM function (39) are critically involved. Although the native DAP molecule is anionic, its active, calcium-decorated form renders it a de facto cationic antimicrobial peptide (CAP) (14, 43). Despite the

general acceptance of the role of CM targeting in the lethal mechanisms of DAP, the relative contributions of the CM, the cell wall (CW), and other targets beyond these sites (e.g., intracellular targets) have not been clearly established (44). The objective of our study was to further elucidate changes in cell surface phenotypes relevant to Dap[r], including CM fluidity, fatty acid content, phospholipid (PL) composition and asymmetry, and surface charge, in a well-known MRSA strain (MW2) after the in vitro selection of DAP resistance by serial passage in sublethal DAP concentrations.

(This work was presented in part at the 48th Annual Interscience Conference on Antimicrobial Agents and Chemotherapy/Infectious Diseases Society of America 46th Annual Meeting, Washington, DC, 25 to 28 October 2008 [abstr. C1-177], a joint meeting of the American Society for Microbiology and the Infectious Diseases Society of America.)

MATERIALS AND METHODS

Bacterial strains. All strains used in this study are listed in Table 1. The parental strain, MW2, is of the USA400 pulsotype. The details of the 20-day serial passage selection process have been previously reported (9). The selective pressure of growth in sublethal concentrations of DAP resulted in the progressive accumulation of single-nucleotide polymorphisms (SNPs) over time that correlated with incremental decreases in DAP susceptibility. The majority of the SNPs resulted in amino acid substitutions (9). The loci affected include *mprF*, encoding lysyl-phosphatidylglycerol (LPG) synthase and translocase (9, 33);

* Corresponding author. Mailing address: LA Biomedical Research Institute at Harbor-UCLA, 1124 West Carson Street, Bldg. RB2, Room 225, Torrance, CA 90502. Phone: (310) 222-6422. Fax: (310) 782-2016. E-mail: abayer@labiomed.org.
[▽] Published ahead of print on 30 March 2009.

TABLE 1. List of strains and their antimicrobial susceptibility
profiles to DAP and vancomycin

Strain	Length of serial passage (days)	Mutation(s)	MIC (μg/ml) of:	
			DAP	VAN[a]
Parental				
CB1118 (MW2)			1	2
Passage set				
CB2201	1	Acetate CoA ligase[b]	1.5	3
CB2202	5	Acetate CoA ligase MprF$_{T345I}$	3	3
CB2203	14	Acetate CoA ligase MprF$_{T345I}$ RpoB$_{I953S}$	6	4
CB2205	20	Acetate CoA ligase MprF$_{T345I}$ RpoB$_{I953S}$ YycG$_{S221P}$	12	4

[a] VAN, vancomycin.
[b] Noncoding region. CoA, coenzyme A.

yycG, encoding a histidine kinase of an operon involved in both CW and CM
metabolism (9, 27); and *rpoB*, the β subunit of RNA polymerase (9). The MICs
of DAP, oxacillin, and vancomycin were determined by using standard procedures for the Etest (AB Biodisc, Dalvagen, Sweden) on Mueller-Hinton agar
(MHA) plates (Difco Laboratories, Detroit, MI). For the DAP Etest, plates were
supplemented with calcium (50 μg/ml CaCl$_2$). Growth curves (24 h) of the strains
in tryptic soy broth (TSB) revealed that the more Dap[r] passage strains (CB2203
and CB2205) grew modestly slower than the parental strain (data not shown).
However, all six strains reached equivalent counts at 24 h (~5 × 10^9 CFU/ml).

Population analysis. The population analysis of a selected strain pair (the
parent strain CB1118 and the 20-day Dap[r] passage mutant CB2205) was carried
out with DAP, oxacillin, and vancomycin by following a standard agar dilution
protocol as previously described (28). DAP population analyses were performed
on calcium-supplemented (50 μg/ml) MHA plates.

CAP susceptibilities. Our prior studies showed that Dap[r] clinical strains exhibited cross-reductions in susceptibility to prototypical mammalian host defense
CAPs of white blood cell (hNP-1) or platelet (tPMP-1) origin (12). To examine
this phenomenon in the current laboratory-derived Dap[r] strain set, we carried
out in vitro susceptibility assays with the same two CAPs. Standard MICs for such
CAPs are not routinely performed, since conventional nutrient medium tends to
mitigate the activity of these peptides; thus, bactericidal assays were carried out
(47). For tPMP-1, a range of 0.5 to 2 μg/ml was used. For hNP-1, a concentration
of 20 μg/ml was used. tPMP-1 was prepared as previously described (46); hNP-1
was purchased from Peptide International (Louisville, KY). Briefly, log-phase *S.
aureus* cells were diluted into the test CAP solutions to achieve the desired final
inoculum (10^3 and 10^5 CFU/ml for tPMP-1 and hNP-1, respectively) (44, 45) and
then incubated at 37°C. At 120 min of exposure, samples were removed and
processed for quantitative culture to assess the extent of killing by each CAP.
Final data were expressed as the means ± standard deviations (SD) of surviving
log$_{10}$CFU/milliliter.

CM fluidity. Fluidity measurements were carried out using the fluorescent
probe 1,6-diphenyl-1,3,5-hexatriene (DPH). The protocol for DPH incorporation into target CMs, the measurement of fluorescence polarization, and the
calculation of the degree of fluorescence polarization (polarization index [PI])
are described in detail elsewhere (a Biotek Model SFM 25 spectrofluorimeter
was used; excitation and emission wavelengths were 360 and 426 nm, respectively, for DPH) (2). An inverse relationship exists between PI values and CM
fluidity (i.e., a lower PI equates to a greater extent of CM fluidity) (2). These
assays were performed a minimum of 10 times for each strain on separate days.

CM fatty acid composition. Fatty acids of total lipids extracted from *S. aureus*
CMs were analyzed using gas-liquid chromatography after conversion to their
methyl ester form as previously described in detail (courtesy of Microbial ID Inc.,
Newark, DE) (2).

Cell surface charge. Poly-L-lysine (PLL) is a polycationic molecule that is used
to study the interactions of CAPs with charged CM bilayers (10, 16). A fluorescein isothiocyanate-labeled PLL binding assay was performed using flow cytometric methods as previously described (using a FACSCalibur; Beckman Instruments, Alameda, CA) (29). Data were expressed as mean fluorescent units
(±SD). The lower the amount of residual cell-associated label, the greater the

PLL repulsion and the more positively charged the *S. aureus* cell envelope (29).
At least three independent runs were performed on separate days.

CW thickness. CW thickness was determined by transmission electron microscopy (EM). Cells were prepared for EM by previously published techniques (21). One
hundred CW thickness measurements were taken from a minimum of 50
bacterial cells for each strain at a magnification of 190,000× (model 100CX;
JEOL, Tokyo, Japan) using digital image capture and morphometric measurement (v54; Advanced Microscopy Techniques, Danvers, MA). The bacterial cells
examined each were in a different field, were intact, were in full cross-section
without a sectioning artifact, and were nondividing. CWs were measured from
the outer aspect of the CM to the outer aspect of the CW. Mean (±SD) CW
thickness then was determined for each strain.

Isolation of RNA. For RNA isolation, fresh overnight cultures of *S. aureus*
strains were used to inoculate TSB to an optical density at 600 nm of 0.1. Cells
were harvested during exponential growth (2 h), early stationary phase (6 h), and
late stationary phase (12 h). Total RNA was isolated from the cell pellets by
using the RNeasy kit (Qiagen, Valencia, CA) and the FASTPREP FP120 instrument (BIO 101, Vista, CA) according to the manufacturers' recommended
protocols.

Northern blot analysis. Northern blot analyses were performed as described
previously, with minor modifications (35). Digoxigenin-labeled DNA probes
were synthesized using a PCR-based digoxigenin probe synthesis kit (Roche)
using primers mprF-F (5′-GTAGTAATCACATTGTATCGGGAGT-3′),
mprF-R (5′-GATGCATCGAAAACATGGAATAC-3′), dlt-F (5′-ATATGATT
GTTGGGATGATTGGTGCCA-3′), and dlt-R (5′-ACATATGGTCCAACTG
AAGCTACG-3′) to synthesize *mprF*- and *dlt*-specific probes, respectively.

CM PL content and PL asymmetry measurements. PLs were extracted from *S.
aureus* by standard methods (7, 29). The three major *S. aureus* PLs, phosphatidylglycerol (PG; negatively charged), cardiolipin (CL; negatively charged), and
LPG (positively charged), were separated by two-dimensional thin-layer chromatography using Silica 60 F254 HPTLC plates (Merck). First-dimension chloroform-methanol–25% ammonium hydroxide (65:25:6, by volume) in the vertical
orientation and second-dimension chloroform:water:methanol:glacial acetic
acid:acetone (45:4:8:9:16, by volume) in the horizontal orientation were used for
the separation of the PLs for further quantitation by phosphate estimation (29).
For quantitative analysis, isolated PLs were digested at 180°C for 3 h with 0.3 ml
70% perchloric acid and quantified spectrophotometrically at an optical density
at 600 nm as previously described (29). At least three independent runs were
performed on separate days.

Fluorescamine, which specifically labels only surface-exposed amino-PLs (i.e.,
outer CM leaflet), was used to assess the CM LPG distribution in the outer and
inner CM bilayers. The protocols of labeling and the quantitative estimation of
PL asymmetry by UV detection, ninhydrin spraying, and chemical analysis were
strictly followed as previously described (12, 29).

Statistical analysis. Data were analyzed by the two-tailed student's *t* test, with
$P < 0.05$ representing a significant difference.

RESULTS

MIC. The Etest MICs are listed in Table 1. As previously
described (9), the DAP MICs progressively increased during
the 20-day serial exposure period, from a MIC of 1 to 32. The
vancomycin MICs increased by one doubling dilution with
sublethal DAP passage from a MIC of 2 to 4 μg/ml during this
same time period. The oxacillin MIC for the parental strain
was 24 μg/ml but was 1.5 μg/ml for the 20-day passage isolate,
exhibiting the see-saw reciprocal phenomenon previously described for vancomycin-intermediate *S. aureus* (VISA) strains
for vancomycin and oxacillin (37, 38).

Population analysis. As expected, the DAP population
curve was shifted to the right in the 20-day mutant (CB2205)
compared to that of the parental strain (CB1118) (data not
shown). This shift corresponds to an increase in the DAP MIC
and reduced oxacillin susceptibility in this population of organisms. In contrast, the oxacillin population curve was shifted to
the left for the mutant (i.e., more oxacillin susceptible), paralleling the MIC data described above and confirming a modest
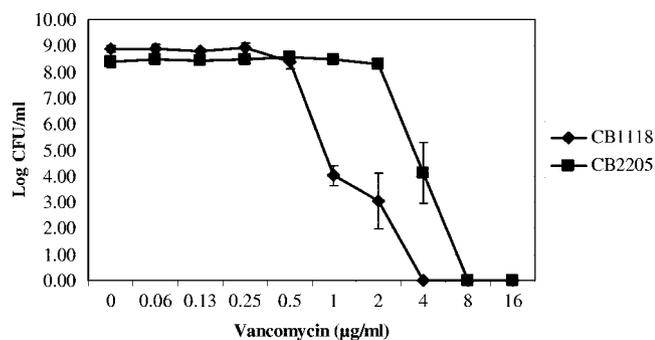reciprocal effect on oxacillin susceptibility (data not shown).

FIG. 1. Population analyses of study strains upon exposure to a range of vancomycin concentrations (conc.). These data represent the means (±SD) for three separate assays.
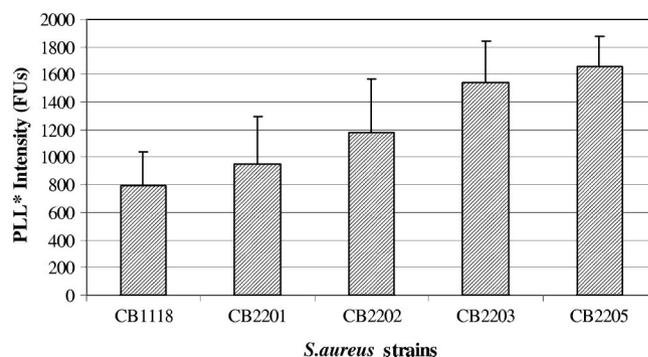

FIG. 2. Net surface charge for the strain set based on fluorescein-isothiocyanate labeled PLL (PLL*) binding. The higher the intensity in fluorescent units (FUs), the more negative the relative surface charge.

Moreover, the vancomycin population curve of the baseline organism already had a subpopulation of VISA isolates, and these also shifted to the right for the Dap^r mutant, which is compatible with its increase in vancomycin MICs into the hetero-VISA range (Fig. 1).

CAP susceptibilities. The Dap^r mutant (CB2205) showed cross-reductions in susceptibilities to the two prototypical mammalian CAPs. For tPMP-1, the parental strain viability was reduced to below the level of detection during the 2-h exposure to concentrations of 0.5 to 2 μg/ml; in contrast, the Dap^r mutant exhibited the survival profile (mean percent survival ± SD) at 0.5, 1, and 2 μg/ml tPMP-1, and similarly for hNP-1, the mean percent survival (±SD) after 2 h of exposure to 20 μg/ml peptide of the parental and Dap^r strain 2205 is shown in Table 2.

CM fluidity. There was a modest, although detectable, decrease of relative CM fluidity (an increasing PI means increasing membrane rigidity) as passage strains (CB2201, CB2202, CB2203, and CB2205) became more Dap^r than the parental strain, CB1118. The PIs from 10 independent measurements were 0.3219 ± 0.0339, 0.3281 ± 0.0421, 0.3267 ± 0.0374, 0.3288 ± 0.0272, and 0.3302 ± 0.0401 for the parental strain and four progressively more Dap^r strains, respectively. As controls for these studies, we included an isogenic strain set, ISP479C (0.3312 ± 0.0122) and ISP479R (0.3119 ± 0.0194), which are known to be less and more fluid, respectively (2).

Cell surface charge. The relative surface charge values of all strains are represented in Fig. 2. As controls for these studies, we used an SA113 strain that is known to exhibit a relatively high surface positive charge compared to that of its isogenic Δdlt knockout variant (32). Unexpectedly, the PLL binding was observed to be higher in the Dap^r strains than in the parental strain. Thus, there was an inverse relationship between DAP resistance and surface charge.

CM fatty acid composition. Fatty acid data for the parental strain and the most Dap^r strain (i.e., CB2205) showed a similar pattern in terms of iso and ante-iso (branched chain) fatty acids, unsaturation indices, and acyl chain length profiles (data not shown).

CW thickness. As shown in Fig. 3, the Dap^r strain has significantly thicker CWs (31.3 ± 2.7 nm) than the parental strain (20.4 ± 2.7 nm; $P < 0.05$).

Expression of genes that affect surface charge (*mprF* and *dlt* operon). It has been shown that the *S. aureus mprF* and *dlt* operon encode proteins that enhance the net positive charge of the cell surface envelope by lysinylating CM PG and alanylating CW teichoic acids, respectively (31, 32, 33, 41). It also has been hypothesized that MprF is responsible for translocating LPG to the outer CM bilayer (23). To determine the transcriptional profiles of these two genes, Northern blot analyses were performed on RNA samples isolated from cultures of CB1118, CB2201, CB2202, CB2203, and CB2205 grown in TSB. As shown in Fig. 4A, *mprF* expression was detected in all five strains during early exponential and stationary growth phases (2 and 12 h). Importantly, the increased levels of *mprF* transcripts were detected in Dap^r strains (CB2202, CB2203, and CB2205) during early exponential growth (2 h). Additionally, *mprF* expression was increased in all four passage strains compared to levels for the parental strain in stationary phase. Similarly to *mprF* expression, the transcription of the *dlt* operon was increased in the three Dap^r strains during early exponential growth (Fig. 4B).

CM PL content and asymmetry measurements. Two-dimensional thin-layer chromatography and LPG-fluorescamine labeling revealed that the total amounts of the positively charged LPG (outer and inner layers) in the CM were higher in the Dap^r strains than in the parental strain. Moreover, there was a progressive upward trend in the proportion of total and outer CM leaflet LPG in the strain set during the in vitro selection of Dap^r strains. The proportions of the other PLs (i.e., PG and CL) were similar among the strains, although as the proportion of LPG increased in the more Dap^r strains, the proportion of PG declined concordantly. Small amounts of CL were detected in these experiments. These data are shown in Table 3.

TABLE 2. In vitro susceptibilities of study strains to CAPs

Strain	% Survival (means ± SD) after 2-h exposure to:			
	0.5 μg/ml tPMP-1	1.0 μg/ml tPMP-1	2.0 μg/ml tPMP-1	20 μg/ml hNP-1
CB1118	ND[a]	ND	ND	68 ± 15
CB2205	105 ± 29	90 ± 26	99 ± 37	105 ± 26

[a] ND, not detected (below the detection level).

20.4 ± 2.7nm   31.3 ± 2.7nm
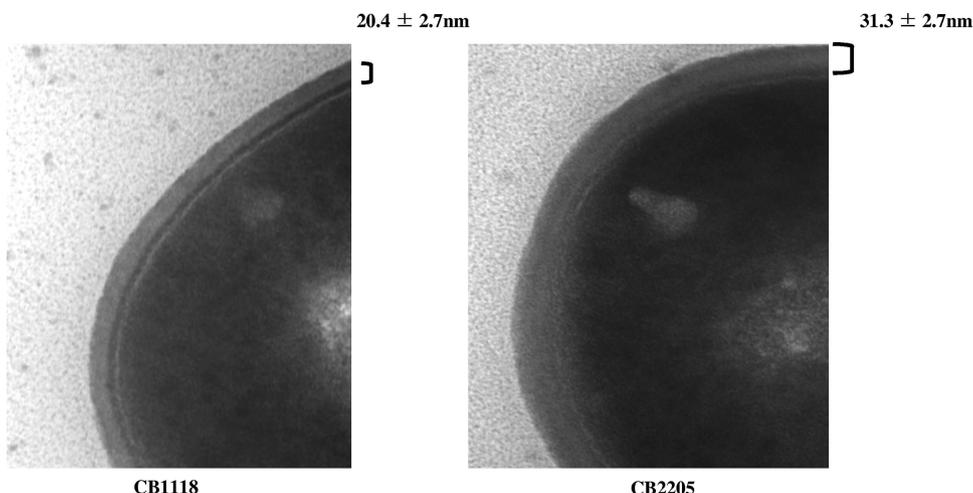

CB1118   **CB2205**

FIG. 3. Transmission EM of the parental strain (CB1118) and Dap[r] mutant (CB2205). The thickness of the CB1118 (20.4 ± 2.7 nm) and CB2205 (31.3 ± 2.7 nm) CWs is indicated.

DISCUSSION

In the context of the rising problems of multidrug resistance among gram-positive pathogens, especially to glycopeptide agents, DAP (lipopeptide) offers an important addition to the antibacterial armamentarium (15). However, examples of the isolation of Dap[r] *S. aureus* strains in association with clinical treatment failure (9, 12, 15) suggest the need for the detailed analysis of the mechanism(s) of resistance of such organisms (12). In the current study, we utilized a well-characterized isogenic MRSA strain set selected for DAP resistance by serial in vitro passage (9) to compare their phenotypic profiles to data we recently published related to a clinically derived *S. aureus* isogenic strain set (12). Since the putative mechanism of action of DAP has focused on CM targeting (12), we characterized a number of key CM properties in this study. As detailed below, the cadre of cell surface and CM perturbations found in the present laboratory-derived strain set were strikingly disparate from those previously documented for Dap[r] strains isolated from recalcitrant clinical infections (12).

Several reports have demonstrated a correlation between decreased oxacillin resistance and a concomitant increase in resistance to vancomycin into the VISA range (the so-called see-saw effect) (37, 38). The mechanism(s) involved in this phenomenon appear to be multifactorial. For example, some studies have implicated the deletion of *mecA* or *mecA* mutations in the presence of vancomycin exposures in the see-saw effect (1, 34, 38). These investigations have suggested an incompatibility between the simultaneous expression of high-level vancomycin resistance and high-level methicillin resistance in MRSA. PBP2a, a *mecA*-encoded protein, is not capable of cross-linking peptidoglycan-containing stem peptide modified by *van* resistance genes (8, 36). Interestingly, we found a similar reciprocal effect, involving increasing DAP resistance and the evolution of the VISA phenotype on the one hand and decreasing oxacillin resistance on the other hand. In contrast, Camargo et al. (4) recently observed that laboratory-derived Dap[r] strains had increased resistance to vancomycin and increased resistance to oxacillin, suggesting strain-specific and/or independent mechanisms of resistance to these agents as related to the induction of the reciprocal phenomenon. For example, relevantly to our current findings, Komatsuzawa et al. (19) described an association between mutations in the *mprF* (*fmtC*) gene and oxacillin resistance in vitro. Thus, it seems reasonable to speculate that the gain-in-function *mprF* SNP as we demonstrated secondarily influences the full expression of the *mecA*-mediated oxacillin resistance phenotype. Taking these results together, the relationship of increasing DAP and vancomycin resistance coincident with decreasing oxacillin resistance in vitro has the following features: (i) relative strain specificity, (ii) a nonrequirement for the presence of DAP (in contrast to vancomycin-oxacillin interactions) (1), and (iii) a mutation in *mprF* as seen in our Dap[r] strains could well influence the expression of oxacillin resistance.

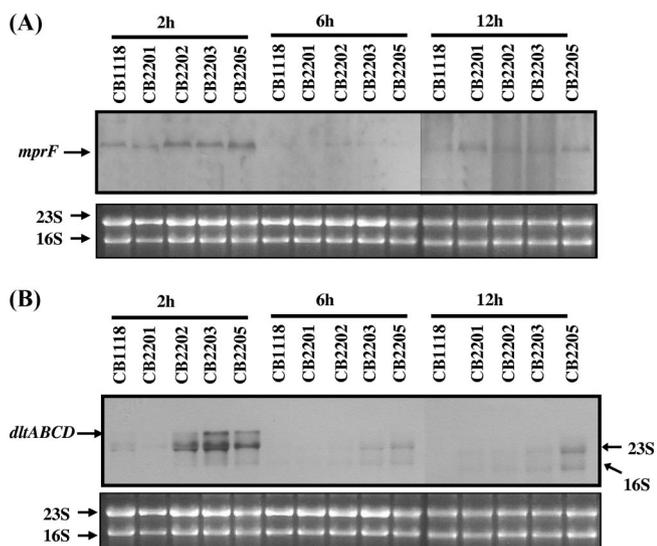One prominent correlate of resistance to the CM-targeting

FIG. 4. (A and B) Northern blot analyses for *mprF* and *dlt* operon expression. Total cellular RNA samples were isolated at 2, 6, and 12 h postinoculation from *S. aureus* cells cultured in TSB.

TABLE 3. PL composition and asymmetry of LPG for the study strains[a]

Strain	% of total PL content (mean ± SD)				
	Inner[b] LPG	Outer[b] LPG	Total LPG	PG	CL
CB1118	**11.16 ± 3.5**	**1.21 ± 0.61**	**12.37 ± 3.3**	**83.96 ± 0.67**	5.38 ± 3.6
CB2201	10.92 ± 2.2	1.37 ± 0.26	12.29 ± 2.0	86.37 ± 3.3	3.60 ± 0.0
CB2202	11.64 ± 2.4	1.70 ± 0.65	13.34 ± 2.1	80.95 ± 4.3	8.59 ± 3.3
CB2203	15.41 ± 2.5	2.56 ± 1.5	17.96 ± 1.1	72.93 ± 6.8	12.70 ± 1.8
CB2205	**18.61 ± 4.4**	**6.00 ± 2.5**	**24.61 ± 3.5**	**70.02 ± 9.1**	7.43 ± 7.8

[a] Substantive differences between the parental strain and the 20-day DAP-nonsusceptible passage mutant are in boldface.
[b] Membrane leaflet.

action of many CAPs is the relative state of CM order (fluidity). Thus, intact CMs or artificial membrane vesicles or bilayers, which are either very fluid or very rigid, tend to be resistant to CAP-induced permeabilization (45). This has led to the notion that for each specific CAP-CM interaction, there is an optimum relative CM order at which individual CAPs exert maximal activity. For example, we previously showed that the CMs of *S. aureus* strains exhibiting in vitro resistance to the platelet CAP tPMP-1 demonstrated significantly more fluid CMs than tPMP-1-susceptible strains (29). Alternatively, rendering such strains as CW-free protoplasts by enzymatic (lysostaphin) CW degradation induced a shift in the CM order toward very rigid CMs, which also was associated with tPMP-1 resistance (45). In our prior investigation of clinically derived Dap[r] strains (12), such organisms tended to have more fluid CMs than the original parental isolate (12). In contrast, in the current study, as in vitro-passaged organisms acquired increasingly Dap[r] phenotypes, their CMs became more rigid. This observation raises a number of possibilities: (i) alterations in CM fluidity are a nonspecific response mechanism in *S. aureus* to many different CAP exposures and are not precisely linked to the CAP-R phenotype; (ii) different CAPs have distinct structure-function relationships that could dictate the nature and scope of CM fluidity shifts associated with peptide resistances; and (iii) in vitro-derived Dap[r] strains are exposed only to a single CAP, while clinically derived Dap[r] strains have been exposed to any number of innate host defense molecules during disseminated endovascular infections (including CAPs such as those from platelets and polymorphonuclear leukocytes) (12, 25). This concept is supported by our recent documentation of cross-resistance in clinical Dap[r] strains to both tPMP-1 and hNP-1 (a prototypic polymorphonuclear leukocyte CAP) (12). It is of interest that despite the lack of exposure to host defense CAPs, the Dap[r] laboratory strain in this study did show reduced killing by the two prototypical CAPs described above. This result suggested that CM perturbations induced by in vitro passage in DAP evoke a generalizable adaptation to unrelated CAPs. The exact mechanism of altered CM fluidity in Dap[r] strains is not well understood, but it does not appear to be linked to shifts in fatty acid unsaturation indices or branched chain species (18).

Another notable feature of clinical Dap[r] strains characterized in our prior investigations was an increased positive surface charge compared to those of their isogenic parenteral strains (12). Since the *mprF* and *dlt* operons are intimately involved in maintaining positive surface charge in *S. aureus*, it follows that mutations in these loci could substantially impact the net surface charge. In our studies of Dap[r] clinical strains, we found an association between *mprF* point mutations and a gain-in-function phenotype (12). This was manifested by the increased translocation of the positively charged PL species LPG to the outer CM leaflet. Gain-in-function MprF alleles in Dap[r] clinical strains also have been seen in other studies (9, 11, 22, 24, 41). This underscored the potential for the charge-mediated surface repulsion of DAP as one explanation for the Dap[r] phenotype. In this context, the present investigation confirmed a gain-in-function MprF allele (associated with both increased synthesis and the translocation of LPG in more progressively Dap[r] strains) as well as enhanced *dlt* operon expression during serial DAP passage. Whether these enhanced *mprF* and *dlt* operon expression profiles are directly related to SNPs or involve other regulatory loci such as *aps/graRS* is not known (6, 42). Interestingly, in the present study, notwithstanding the increased expression profiles of *dlt* and *mprF* and phenotypic gains in function, the net surface charge paradoxically became less positive during in vitro Dap[r] selection. This suggested the intriguing concept that other surface factors significantly contribute to the net envelope charge. The principal candidate in this regard would be the extent of CW glutamate amidation, which previously has been linked to glycopeptide resistance in MRSA VISA strains (22). The observation of thickened CWs among the Dap[r] isolates in this investigation supports such a paradigm. Thus, taken together, the enhanced negative surface charge in the in vitro-selected Dap[r] strains could conceivably facilitate rapid early DAP surface binding, while the specific upregulation of *mprF* function and/or the increased CM rigidity in these strains subsequently could elicit a CM-specific DAP repulsion. Such a sequence of events then would collectively read out as reduced DAP binding.

It is important to point out that increased CW thickness has been associated with both the Dap[r] and VISA phenotype in two studies (4, 5). Although postulated to be an affinity-trapping mechanism for Dap, as documented for vancomycin in VISA isolates (5), this mechanism has not been confirmed to date. Moreover, as for VISA strains, the thickened CW phenotype also may be related to altered CW synthesis or perturbed autolytic pathways (5). Further, it also is possible that the CW thickening is merely a nonspecific secondary adaptive response to a primary alteration in CM fluidity or function (5, 15). Of note, we demonstrated thickened CWs in our Dap[r] mutant in association with the VISA phenotype by both MIC testing and population analysis, despite the organism never being exposed to vancomycin. This same phenomenon was

demonstrated recently by Camargo et al. (4) utilizing a different *S. aureus* laboratory strain. Thus, the Dap[r] and VISA phenotypes may well share common genotypic and/or metabolic mechanisms in some strain backgrounds; this issue is being actively investigated. Current studies are examining the CW muropeptide, O-acetylation, and amidation profiles of this strain set to provide more clarity into our findings (13).

Finally, since DAP appears to be a CM-targeting agent, the bioenergetic state of the CM may well impact DAP susceptibility (3, 20). Kaatz et al. (15) evaluated a clinical Dap[r] isolate from a patient with MRSA tricuspid endocarditis and noted (i) reduced DAP binding to their whole cells and CMs, (ii) reduced CM potential, and (iii) the loss of an 81-kDa CM protein ascribed to have a putative DAP chaperone function. Silverman et al. (40) also have noted altered CM energetics among in vitro-selected Dap[r] strains. Although this was not assessed in the present investigation, our recent analysis of CM potential in clinical Dap[r] strains did not identify any abnormalities (12).

In summary, the mechanism(s) and pathways underlying the in vitro-selected Dap[r] phenotype in MW2 (USA400) appear to be both multifactorial and distinct from those seen in clinically derived strains. Whether the progressive accumulation of SNPs in genes such as *mprF*, *yycFG*, *rpoB*, and *rpoC*, which potentially are associated with gains in function, drive the Dap[r] phenotypes or are just surrogate secondary markers remains to be elucidated. It also will be important to determine whether the CM and CW perturbations we observed in strain MW2 (USA400) are strain specific or are definable in other pulsotypes.

ACKNOWLEDGMENTS

REFERENCES

1. **Adhikari, R. P., G. C. Scales, K. Kobayashi, J. M. B. Smith, B. Berger-Bachi, and G. M. Cook.** 2004. Vancomycin-induced deletion of the methicillin resistance gene *mecA* in *Staphylococcus aureus*. J. Antimicrob. Chemother. **54:**360–363.
2. **Bayer, A. S., R. Prasad, J. Chandra, A. Koul, A. Verma, R. A. Skurray, N. Firth, M. Brown, S.-P. Koo, and M. R. Yeaman.** 2000. In vitro resistance of *Staphylococcus aureus* to thrombin-induced microbicidal protein is associated with alterations in membrane fluidity. Infect. Immun. **68:**3548–3553.
3. **Bayer, A. S., P. J. McNamara, M. R. Yeaman, L. I. Kupferwasser, N. Lucindo, T. Jones, H.-G. Sahl, and R. A. Proctor.** 2006. Disruption of the complex I NADH oxido-reductase gene (*snoD*) in *Staphylococcus aureus* is associated with reduced susceptibility to the microbicidal activity of thrombin-induced platelet microbicidal protein-1. J. Bacteriol. **188:**211–222.
4. **Camargo, I. L. Baratella da Cunha, H.-M. Neoh, L. Cui, and K. Hiramatsu.** 2008. Serial daptomycin selection generates daptomycin-nonsusceptible *Staphylococcus aureus* with a hetero-VISA phenotype. Antimicrob. Agents Chemother. **52:**4289–4299.
5. **Cui, L., E. Tominaga, H. M. Neoh, and K. Hiramatsu.** 2006. Correlation between reduced daptomycin susceptibility and vancomycin resistance in vancomycin-intermediate *Staphylococcus aureus*. Antimicrob. Agents Chemother. **50:**1079–1082.
6. **Dirk, K., S. Herbert, S. A. Kristian, A. Khosravi, V. Nizet, F. Götz, and A. Peschel.** 2008. The GraRS regulatory system controls *Staphylococcus aureus* susceptibility to antimicrobial host defenses. BMC Microbiol. **8:**85.
7. **Dixit, B. L., and C. M. Gupta.** 1998. Role of the actin cytoskeleton in regulating the outer phosphatidylethanolamine levels in yeast plasma membrane. Eur. J. Biochem. **254:**202–206.
8. **Fox, P. M., R. J. Lampen, K. S. Stumpf, G. L. Archer, and M. W. Climo.** 2006. Successful therapy of experimental endocarditis caused by vancomycin-resistant *Staphylococcus aureus* with a combination of vancomycin and beta-lactam antibiotics. Antimicrob. Agents Chemother. **50:**2951–2956.
9. **Friedman, L., J. D. Adler, and J. A. Silverman.** 2006. Genetic changes that

10. correlate with reduced susceptibility to daptomycin in *Staphylococcus aureus*. Antimicrob. Agents Chemother. **50:**2137–2145.
10. **Hartmann, W., and H. J. Galla.** 1978. Binding of polylysine to charged bilayer membranes: molecular organization of a lipid peptide complex. Biochim. Biophys. Acta **509:**474–490.
11. **Ichihashi, N., K. Kurokawa, M. Matsuo, C. Kaito, and K. Sekimizu.** 2003. Inhibitory effects of basic or neutral phospholipid on acidic phospholipid-mediated dissociation of adenine nucleotide bound to DnaA protein, the initiator of chromosomal DNA replication. J. Biol. Chem. **278:**28778–28786.
12. **Jones, T., M. R. Yeaman, G. Sakoulas, S.-J. Yang, R. A. Proctor, H.-G. Sahl, J. Schrenzel, Y. Q. Xiong, and A. S. Bayer.** 2008. Failures in clinical treatment of *Staphylococcus aureus* infection with daptomycin are associated with alterations in surface charge, membrane phospholipid asymmetry, and drug binding. Antimicrob. Agents Chemother. **52:**269–278.
13. **Julian, K., K. Kosowska-Shick, C. Whitener, M. Roos, H. Labischinski, A. Rubio, L. Parent, L. Ednie, L. Koeth, T. Bogdanovich, and P. C. Appelbaum.** 2007. Characterization of a daptomycin-nonsusceptible vancomycin-intermediate *Staphylococcus aureus* strain in a patient with endocarditis. Antimicrob. Agents Chemother. **59:**3445–3448.
14. **Junga, D., J. P. Powers, Suzana K. Straus, B., and R. E. W. Hancock.** 2008. Lipid-specific binding of the calcium-dependent antibiotic daptomycin leads to changes in lipid polymorphism of model membranes. Chem. Phys. Lipids **154:**120–128.
15. **Kaatz, G. W., T. S. Lundstrom, and S. M. Seo.** 2006. Mechanisms of daptomycin resistance in *Staphylococcus aureus*. Int. J. Antimicrob. Agents **28:**280–287.
16. **Kim, J., M. Mosior, L. A. Chung, H. Wu, and S. McLaughlin.** 1991. Binding of peptides with basic residues to membranes containing acidic phospholipids. Biophys. J. **60:**135–148.
17. **Kirkpatrick, P., A. Raja, J. LaBonte, and J. Lebbos.** 2003. Daptomycin. Nat. Rev. Drug. Discov. **2:**943–944.
18. **Klein, W., M. H. Weber, and M. A. Marahiel.** 1999. Cold shock response of *Bacillus subtilis*: isoleucine-dependent switch in the fatty acid branching pattern for membrane adaptation to low temperatures. J. Bacteriol. **181:**5341–5349.
19. **Komatsuzawa, H., K. Ohta, T. Fujiwara, G. H. Choi, H. Labischinski, and M. Sugai.** 2001. Cloning and sequencing of the gene, *fmtC*, which affects oxacillin resistance in methicillin-resistant *Staphylococcus aureus*. FEMS Microbiol. Lett. **203:**49–54.
20. **Koo, S.-P., A. S. Bayer, H.-G. Sahl, R. A. Proctor, and M. R. Yeaman.** 1996. Staphylocidal action of thrombin-induced platelet microbicidal protein is not solely dependent on intact transmembrane potential. Infect. Immun. **64:**1070–1074.
21. **Koo, S.-P., M. R. Yeaman, C. C. Nast, and A. S. Bayer.** 1997. The cytoplasmic membrane is a primary target for the staphylocidal action of thrombin-induced platelet microbicidal protein. Infect. Immun. **65:**4795–4800.
22. **Kraus, D., H. Kalbacher, J. Buschmann, B.-B. Bachi, F. Gotz, and A. Peschel.** 2007. Muropeptide modification-amidation of peptidoglycan D-glutamate does not affect the proinflammatory activity of *Staphylococcus aureus*. Infect. Immun. **75:**2084–2087.
23. **Kraus, D., C. Ernst, and A. Peschel.** 2008. Characterization of the *Staphylococcus aureus* defensin resistance factor, MprF, abstr. 535. Abstr. 13th Int. Symp. Staphylococci Staphylococcal Infect., Cairns, Australia.
24. **Kristian, S. A., M. Durr, J. A. Van Strijp, B. Neumeister, and A. Peschel.** 2003. MprF-mediated lysinylation of phospholipids in *Staphylococcus aureus* leads to protection against oxygen-independent neutrophil killing. Infect. Immun. **71:**546–549.
25. **Kupferwasser, L. I., M. R. Yeaman, S. M. Shapiro, C. C. Nast, and A. S. Bayer.** 2002. In vitro susceptibility to thrombin-induced platelet microbicidal protein is associated with reduced disease progression and complication rates in experimental *Staphylococcus aureus* endocarditis; histopathologic, and echocardiographic analyses. Circulation **105:**746–752.
26. **Lowy, F. D.** 1998. *Staphylococcus aureus* infections. N. Engl. J. Med. **339:**520–532.
27. **Mohedano, M. L., K. Overfweg, A. de la Fuente, M. Reuter, S. Altabe, F. Mulholland, D. de Mendoza, P. Lopez, and J. M. Wells.** 2005. Evidence that the essential regulator YycF in *Streptococcus pneumoniae* modulates expression of fatty acid biosynthesis genes and alters membrane composition. J. Bacteriol. **187:**2357–2367.
28. **Moore, M. R., F. Perdreau-Remington, and H. F. Chambers.** 2003. Vancomycin treatment failure associated with heterogeneous vancomycin-intermediate *Staphylococcus aureus* in a patient with endocarditis and in the rabbit model of endocarditis. Antimicrob. Agents Chemother. **47:**1262–1266.
29. **Mukhopadhyay, K., W. Whitmire, Y. Q. Xiong, J. Molden, A. Peschel, P. J. McNamara, R. A. Proctor, M. R. Yeaman, and A. S. Bayer.** 2007. Reduced in vitro susceptibility of *Staphylococcus aureus* to thrombin-induced platelet microbicidal protein-1 (tPMP-1) is associated with alterations in cell membrane phospholipid composition and asymmetry. Microbiology **153:**1187–1197.
30. **Muthaiyan, A., J. A. Silverman, R. K. Jayaswal, and B. J. Wilkinson.** 2008. Transcriptional profiling reveals that daptomycin induces the *Staphylococcus*

aureus cell wall stress stimulon and genes responsive to membrane depolarization. Antimicrob. Agents Chemother. **52:**980–990.

31. **Oku, Y., K. Kurokawa, N. Ichihashi, and K. Sekimizu.** 2004. Characterization of the *Staphylococcus aureus mprF* gene, involved in lysinylation of phosphatidylglycerol. Microbiology **150:**45–51.

32. **Peschel, A., M. Otto, R. W. Jack, H. Kalbacher, G. Jung, and F. Gotz.** 1999. Inactivation of the *dlt* operon in *Staphylococcus aureus* confers sensitivity to defensins, protegrins, and other antimicrobial peptides. J. Biol. Chem. **274:**8405–8410.

33. **Peschel, A., R. W. Jack, M. Otto, L. V. Collins, P. Staubitz, G. Nicholson, H. Kalbacher, W. F. Nieuwenhuizen, G. Jung, A. Tarkowski, K. P. van Kessel, and J. A. van Strijp.** 2001. *Staphylococcus aureus* resistance to human defensins and evasion of neutrophil killing via the novel virulence factor MprF is based on modification of membrane lipids with L-lysine. J. Exp. Med. **193:**1067–1076.

34. **Reipert, A., K. Ehlert, T. Kast, and G. Bierbaum.** 2003. Morphological and genetic differences in two isogenic *Staphylococcus aureus* strains with decreased susceptibilities to vancomycin. Antimicrob. Agents Chemother. **47:**568–576.

35. **Rice, K. C., T. Patton, S. J. Yang, A. Dumoulin, M. Bischoff, and K. W. Bayles.** 2004. Transcription of the *Staphylococcus aureus cid* and *lrg* murein hydrolase regulators is affected by sigma factor B. J. Bacteriol. **186:**3029–3037.

36. **Severin, A., S. W. Wu, K. Tabei, and A. Tomasz.** 2004. Penicillin-binding protein2 is essential for expression of high-level vancomycin resistance and cell wall synthesis in vancomycin-resistant *Staphylococcus aureus* carrying the enterococcal *vanA* gene complex. Antimicrob. Agents Chemother. **48:**4566–4573.

37. **Sieradzki, K. T. Leski, J. Dick, L. Borio, and A. Tomasz.** 2003. Evolution of a vancomycin-intermediate *Staphylococcus aureus* strain in vivo: multiple changes in the antibiotic resistance phenotypes of a single lineage of methicillin-resistant *S. aureus* under the impact of antibiotics administered for chemotherapy. J. Clin. Microbiol. **41:**1687–1693.

38. **Sieradzki, K., and A. Tomasz.** 1997. Inhibition of cell wall turnover and autolysis by vancomycin in a highly vancomycin-resistant mutant of *Staphylococcus aureus*. J. Bacteriol. **179:**2557–2566.

39. **Silverman, J. A., N. Oliver, O. Andrew, and T. Li.** 2001. Resistance studies with daptomycin. Antimicrob. Agents Chemother. **45:**1799–1802.

40. **Silverman, J. A., N. G. Perlmutter, and H. M. Shapiro.** 2003. Correlation of daptomycin bactericidal activity and membrane depolarization in *Staphylococcus aureus*. Antimicrob. Agents Chemother. **47:**2538–2544.

41. **Staubitz, P., A. Peschel, W. F. Nieuwenhuizen, M. Otto, F. Gotz, G. Jung, and R. W. Jack.** 2001. Structure-function relationships in the tryptophan rich, antimicrobial peptide indolicidin. J. Pept. Sci. **7:**552–564.

42. **Staubitz, P., H. Neumann, T. Schneider, I. Wiedemann, and A. Peschel.** 2004. MprF-mediated biosynthesis of lysylphosphatidylglycerol, an important determinant in staphylococcal defensin resistance. FEMS Microbiol. Lett. **231:**67–71.

43. **Tally, F. P., M. Zeckel, M. M. Wasilewski, C. Carini, C. L. Berman, G. L. Drusano, and F. B. Oleson Jr.** 1999. Daptomycin: a novel agent for gram-positive infections. Expert Opin. Investig. Drugs **8:**1223–1238.

44. **Xiong, Y. Q., A. S. Bayer, and M. R. Yeaman.** 2002. Inhibition of intracellular macromolecular synthesis in *Staphylococcus aureus* by thrombin-induced platelet microbicidal proteins. J. Infect. Dis. **185:**348–356.

45. **Xiong, Y. Q., K. Mukhopadhyay, M. R. Yeaman, J. Adler-Moore, and A. S. Bayer.** 2005. Functional interrelationships between cell membrane and cell wall in antimicrobial peptide-mediated killing of *Staphylococcus aureus*. Antimicrob. Agents Chemother. **49:**3114–3121.

46. **Yeaman, M. R., K. D. Gank, A. S. Bayer, and E. P. Brass.** 2002. Synthetic peptides that exert antimicrobial activities in whole blood and blood-derived matrices. Antimicrob. Agents Chemother. **46:**3883–3891.

47. **Yount, N. Y., K. D. Gank, Y. Q. Xiong, A. S. Bayer, T. Pender, W. H. Welch, and M. R. Yeaman.** 2004. Platelet microbicidal protein 1: structural themes of a multifunctional antimicrobial peptide. Antimicrob. Agents Chemother. **48:**4395–4404.